Journal of Marine Science and Application (2026) 25: 1490-1499
https://doi.org/10.1007/s11804-025-00726-0

RESEARCH ARTICLE

Hybrid Optimization of Deep-Sea Acoustic Sensor Network Topology for Enhancing Resilience

Wenmin Lin[1,2], Shuaifeng Hao[1,2], Dongsheng Chen[1,2], Feng Tong[1,2] and Peichen Niu[1,2]

Received: 14 March 2025 / Accepted: 20 June 2025
© Harbin Engineering University and Springer-Verlag GmbH Germany, part of Springer Nature 2026

Abstract

In recent years, deep-sea acoustic sensor networks (DSASNs) have gained considerable attention in areas such as deep-sea resource exploration, environmental monitoring, and underwater construction. However, due to the combined effects of adverse DSA channel conditions, a hostile deep-sea environment, long propagation delays, and limited energy supply, DSASNs often experience random performance fluctuations and low resilience. These issues are typically caused by unstable connectivity and abnormal node failures. Given the critical role of network topology in influencing network behavior, this paper proposes a hybrid topology optimization algorithm for DSASNs. The algorithm integrates the virtual force algorithm (VFA) and particle swarm optimization (PSO), leveraging the global search capability of PSO and the local optimization strength of VFA to provide a highly robust solution for improving the DSASN resilience (DSR–VFPSO). Specifically, a comprehensive objective function is formulated to transform the high-resilience topology optimization problem into a dual-objective function of maximizing coverage and optimizing betweenness centrality. This objective is addressed iteratively through the combined use of VFA and PSO to reach an optimal solution. Simulation results reveal that the proposed algorithm effectively improves the resilience of DSASNs under artificial stress conditions caused by random node failures.

Keywords Topology optimization; Resilience; Deep-sea; Underwater acoustic; Shadow zones; Virtual force

1 Introduction

Underwater sensor networks face several challenges, including limited bandwidth, high propagation delays, complex three-dimensional topologies, and strict power constraints. Traditional communication methods, such as radio and optical waves, are generally unsuitable for underwater use due to considerable signal attenuation in seawater (Awan et al., 2019). In contrast, acoustic communication offers better performance in underwater environments because it suffers less attenuation in seawater. Underwater acoustic wireless sensor networks (UAWSNs) employ acoustic signals to establish communication links between spatially distributed sensor nodes. These networks are envisioned to support a wide range of applications, including oceanographic data collection, pollution monitoring, offshore resource exploration, disaster prevention, assisted navigation and tactical surveillance (Akyildiz et al., 2005).

In recent years, with advancements in communication technology, research in underwater acoustic communication has gradually shifted from short-range, high-speed communication in shallow waters to long-range, robust communication in deep-sea environments (Li et al., 2024). This transition has brought deep-sea acoustic sensor networks (DSASNs) to the forefront of research. Unlike shallow-sea environments, the deep sea exhibits notable ocean stratification and different sound propagation modes. The sound speed gradient in the deep sea markedly changes during propagation, resulting in various sound propagation modes such as channel axis, surface channel, shadow zones, and convergence zones (Zhao et al., 2024). Further-

Article Highlights

- A hybrid topology optimization algorithm is developed to improve the resilience of deep-sea acoustic networks by transforming the objective of resiliency enhancement into the optimization of network coverage and betweenness centrality.
- The characteristics of deep-sea acoustic channels are integrated into the algorithm design and network model to enable performance evaluation and comparison in deep-sea scenarios.
- The effectiveness of the proposed algorithm is verified through deep-sea network simulations using artificial node expirations to mimic the impact of adverse environmental conditions on network resilience.

✉ Dongsheng Chen
dschen@xmu.edu.cn

[1] College of Ocean and Earth Sciences, Xiamen University, Xiamen 361100, China

[2] National and Local Joint Engineering Research Center for Navigation and Location Service Technology, Xiamen University, Xiamen 361100, China

more, DSASNs face unique challenges such as node sparsity and severe signal attenuation. Physical damage or interference to network nodes can lead to substantial performance fluctuations due to the diverse acoustic propagation modes and sparse distribution of nodes in deep-sea environments. This phenomenon results in poor network resilience and, in extreme cases, can cause the collapse or complete failure of the network. Therefore, enhancing the resilience of DSASNs has become an urgent and critical issue.

Network resilience is defined as the capability of a network to provide and maintain an acceptable level of service despite various failures and normal operational challenges (Sterbenz et al., 2014). The main goal of resilience is to develop fault-tolerant networks (Huang et al., 2015), which are characterized by robustness and survivability.

Network topology is generally a crucial factor in determining a network's energy consumption, capacity, and reliability (Akyildiz et al., 2005), which can also serve as an important criterion for assessing resilience.

Current research in underwater sensor networks predominantly focuses on optimizing coverage, connectivity, and energy consumption. For instance, Liu et al. (2019) proposed a distributed node deployment algorithm based on virtual forces, which effectively enhances network coverage, optimizes energy consumption, and improves node distribution. Yan et al. (2021) introduced a growth ring style uneven node depth-adjustment self-deployment optimization algorithm aimed at improving coverage and reliability, addressing the energy hole problem, and extending the network's life cycle. Additionally, Choudhary et al. (2021) developed a dynamic topology algorithm for node deployment to maintain network coverage and connectivity while reducing energy consumption. Their approach demonstrated an increase in residual energy by 3% and 18% compared to other existing algorithms.

Given the NP-hard nature of underwater topology optimization, bio-inspired algorithms, such as particle swarm optimization (PSO), ant colony algorithm, and genetic algorithm (GA), have demonstrated better performance in underwater wireless sensor networks (Vihman et al., 2021). Recent algorithmic innovations further highlight the effectiveness of swarm intelligence. For example, Kumar Gola et al. (2021) introduced a sea lion optimization algorithm that achieved a 95% connectivity ratio across varying numbers of acoustic sensor nodes. Similarly, a krill herd-based deployment strategy by Dong et al. (2023) and a multi-population firefly algorithm by Annapurna and Sudhir (2023) focused on topology optimization with an emphasis on energy consumption, both yielding promising results.

However, the harsh deep-sea environment, characterized by node vulnerability and the risk of cascading failures, necessitates resilience-focused solutions. Yuan et al. (2024) established through cascading failure modeling that node deployment distance plays a critical role in determining network invulnerability. Aiming to enhance fault tolerance against random node failures, Dong et al. (2022) introduced classic scale-free structures into underwater acoustic sensor networks (UASNs). Additionally, Xu et al. (2023) proposed an efficient deployment scheme, EDNPM, which specifically considers reliable data transmission to improve network resilience. Extensive experiments have demonstrated that EDNPM outperforms other deployment algorithms in terms of network performance and robustness under various network settings. Chi et al. (2023) proposed a flexibility-based network topology evaluation model (FEM), and further developed a reinforcement learning-based model, FEM–DRL. This model enables nodes to flexibly maintain an optimal topology structure even in harsh underwater environments, thereby notably improving network resilience. Despite these advancements, research based on the deep-sea environment remains largely unexplored. Aiming to address this gap, a hybrid algorithm that integrates the virtual force algorithm (VFA) with PSO and is specifically designed for the pre-deployment static optimization of DSASNs to improve thre resilience of networks, which called DSR–VFPSO, is proposed. This approach leverages the global search capability of PSO alongside the local optimization strength of VFA, transforming resilience-oriented topology optimization into a multi-objective problem that balances network coverage and betweenness centrality (BC). The resilience evaluation framework developed in this study assesses network performance based on post-failure connectivity retention, coverage maintenance, and energy efficiency, metrics that are discussed in detail in Sections 2 and 3.

2 Network model

2.1 Sink-Node network model

The Sink-Node network model is characterized by a centralized sink node that serves as the primary hub for data aggregation and processing across the entire network.

In this model, the sink node is assumed to possess superior computational capabilities and an effectively unlimited energy supply. Any node that fails to establish either a single-hop or multi-hop communication path to the sink node is considered functionally disconnected from the network.

The centrality of the sink node creates heterogeneous node importance across the network. The importance of nodes in the network is assessed using the BC parameter. The formulation follows Freeman's definition as presented below (Freeman, 1977).

$$\mathrm{BC}_i = \sum_{j,k \in N} \frac{n_{jk}(i)}{n_{jk}} \tag{1}$$

where N represents the number of nodes in the network, n_{jk} denotes the total number of shortest paths between j and k, and $n_{jk}(i)$ is the number of shortest paths between j and k that pass through node i.

In the Sink-Node network, as previously mentioned, the destination for all common nodes is the sink node. Therefore, the formula can be modified as follows to adapt to the requirements.

$$\mathrm{BC}_i = \sum_{j \in N} \frac{n_j(i)}{n_j} \tag{2}$$

where N represents the number of common nodes in the sink-node network, n_j is the number of shortest paths between j and sink node, and $n_j(i)$ denotes the number of shortest paths between$j$and sink node that pass through node i.

2.2 Sensing model

The 0/1 sensing model is a commonly used sensing model in UASNs (Sandeep and Kumar, 2017). Its mathematical expression is given by Eq. (3), where c_{ij} refers to the probability that i perceives j, and d_{ij} represents the Euclidean distance between i and j.

$$c_{ij} = \begin{cases} 1, & d_{ij} \leqslant r \\ 0, & d_{ij} > r \end{cases} \tag{3}$$

Within a circular area centered on the sensor node with a specific sensing radius r, the perception probability is 1; outside this area, the perception probability is 0.

However, the underwater propagation of acoustic signals is subject to refraction due to depth-dependent variations in sound speed, which can lead to the formation of "shadow zones". These areas demonstrate the propagation of minimal signal energy. Thus, communication with a receiver located within a shadow zone can be increasingly challenging (Preisig, 2007). This phenomenon is particularly pronounced in deep-sea environments, where a receiving node resides within the nominal sensing radius of a transmitter, yet effective connectivity cannot be established if the receiver falls within the transmitter's shadow zone. This study enhances the conventional 0/1 sensing model by incorporating shadow zone constraints. Two nodes are considered connected only if the receiving node lies within the perception range of the sending node and is located outside its shadow zone. The formula is mathematically expressed in Eq. (4), where TL_{ij} denotes the transmission loss from i to j.

$$c_{ij} = \begin{cases} 1, & d_{ij} \leqslant r \text{ and } \mathrm{TL}_{ij}, \mathrm{TL}_{ji} \neq \infty \\ 0, & d_{ij} > r \text{ and } \left(\mathrm{TL}_{ij} = \infty \vee \mathrm{TL}_{ji} = \infty\right) \end{cases} \tag{4}$$

2.3 Energy consumption model

In UASNs, data often needs to be transmitted multiple times to ensure reliable transmission. For static UASNs, where nodes do not move, energy consumption primarily results from data transmission and reception. Therefore, the energy consumption of a node can be expressed as follows (Hong et al., 2018):

$$\begin{aligned} E &= E_{tx} + E_{rx} \\ E_{tx} &= \frac{l}{R_b} \times \left(E_{\mathrm{elec_}s} + P_t\right) \\ E_{rx} &= \frac{l}{R_b} \times E_{\mathrm{elec_}r} \end{aligned} \tag{5}$$

where E_{tx} and E_{rx} represent the energy expended to transmit and receive $l-$ bits data, respectively. $E_{\mathrm{elec_}s}$ and $E_{\mathrm{elec_}r}$ refer to the power consumption of transmitting and receiving circuits, respectively (unit: W). R_b and P_t represent the transmission rate and transmission power, respectively.

Aiming to ensure that the receiver can successfully receive the data transmitted by the sender, the required signal power at the receiver P_r can be calculated using the following formula:

$$\begin{aligned} P_r &= \mathrm{SNR} \times P_n \\ P_n &= k \times T \times \mathrm{BW} \end{aligned} \tag{6}$$

where SNR refers to the signal-to-noise ratio, P_n refers to the noise power, k represents the Boltzmann constant, T refers to the absolute temperature in water, BW represents the frequency bandwidth.

The transmitted power can be expressed as follows:

$$P_t = P_r + L_p \tag{7}$$

where P_r refers to the signal power required by the receiver, and L_p refers to the transmission loss, including geometric expansion and absorption losses.

Based on the above discussion, the energy consumption of nodes can be expressed as shown in Eq. (8).

$$E = \frac{l}{R_b} \times \left(E_{\mathrm{elec_}s} + \left(\mathrm{SNR} \times k \times T \times \mathrm{BW} + L_p\right) + E_{\mathrm{elec_}r}\right) \tag{8}$$

3 Algorithm introduction

In this study, a hybrid optimization algorithm called DSR–VFPSO is proposed. As illustrated in Figure 1, the workflow comprises the following two principal phases:

Initialization parameters: configure swarm parameters and environmental constraints;

Iterative optimization: updates the parameters iteratively according to the fitness function until the optimal solution is achieved.

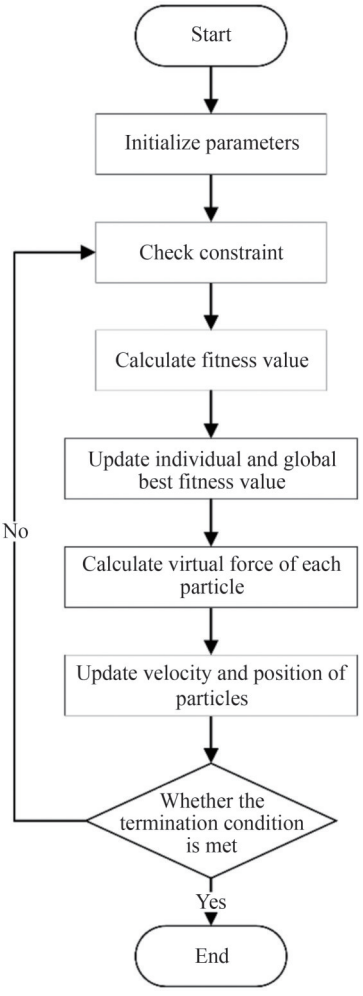


Figure 1 Flow chart of DSR–VFPSO

3.1 Basic principle

The effectiveness of combining VFA and PSO has been verified in previous related studies (Sun et al., 2020; Hu et al., 2022). Therefore, this study will not elaborate on the principles of the algorithm. The velocity and position update formula of the VFPSO hybrid algorithm can be described as follows (Wang et al., 2007):

$$\begin{aligned} \boldsymbol{V}_i(t+1) &= \omega \cdot \boldsymbol{V}_i(t) + c_1 \cdot r_1 \cdot \left(p_{i,\text{best}}(t) - \boldsymbol{X}_i(t)\right) + \\ & c_2 \cdot r_2 \cdot \left(g_{\text{best}}(t) - \boldsymbol{X}_i(t)\right) + c_3 \cdot r_3 \cdot \boldsymbol{vf}_i(t) \\ \boldsymbol{X}_i(t+1) &= \boldsymbol{X}_i(t) + \boldsymbol{V}_i(t+1) \end{aligned} \tag{9}$$

The first three terms of the velocity update formula are consistent with the original PSO algorithm, while the third term is new. Let $\boldsymbol{V}_i$ and $\boldsymbol{X}_i$ represent the ith velocity and position, respectively, and $p_{i,\text{best}}$ denotes the ith best position. ω represents the inertia weight, which is adjusted to balance global convergence and convergence speed. c_1 represents the individual learning factor, c_2 denotes the group learning factor, and c_3 is an acceleration element. r_1, r_2, and r_3 are random numbers between [0, 1], which introduce randomness into the search process and prevent particles from falling into local optimality. $\boldsymbol{vf}_i(t)$ represents the proleptic motion indicated by the virtual force of the ith particle, which is computed using the following expression (Wang et al., 2007):

$$\boldsymbol{vf}_i = \frac{\vec{\boldsymbol{F}}_i}{\left|\vec{\boldsymbol{F}}_i\right|} \times \text{MaxStep} \times e^{-\frac{1}{\left|\vec{\boldsymbol{F}}_i\right|}} \tag{10}$$

where MaxStep is the maximum mobile distance, and $\vec{\boldsymbol{F}}_i$ refers to the resultant force exerted on i. $\vec{\boldsymbol{F}}_i$ can be calculated according to Liu et al. (2019).

3.2 Constraint condition

Connectivity is a critical property that determines the proper detection and communication of events of interest in UAWSN, especially due to the unstable underwater environment (Sandeep and Kumar, 2017). This condition is equally true in deep-sea environments. Thus, in this paper, full connectivity of the network is treated as a constraint.

The network model used in this study is the sink-node network model, as previously mentioned, where full connectivity means that all common nodes must be connected to the sink node, either through single-hop or multi-hop communication.

The sound fields around nodes at different depths vary. Thus, a node is considered properly connected to the sink node only data can be transmitted either uplink or downlink. The connectivity rate r_{con} of the sink-node network can be calculated using Eq. (11).

$$r_{\text{con}} = \frac{n_{\text{con}}}{n} \tag{11}$$

The connectivity rate r_{con} of the sink-node network must be 1, that is, the constraint condition of DSR–VFPSO. In this equation, n_{con} represents the number of nodes that can be connected to the sink node through single-hop or multi-hop communication and $n$represents the number of common nodes in the network.

3.3 Fitness function

In DSR–VFPSO, the primary goal of the proposed algorithm is to improve network resilience. The fitness function is designed to optimize two key objectives: coverage and BC.

Coverage reflects the initial coverage capability of the network at the time of deployment and serves as the basis for overall network performance. Under the constraint of

full connectivity, when aiming to improve resilience or other performance metrics, maintaining the basic performance of the network is crucial.

The three-dimensional space is divided into several cubes when calculating the coverage rate of the network. If all the vertices of a cube are covered by at least one node, then the cube is considered to be covered. The schematic of the coverage rate calculation is shown in Figure 2.

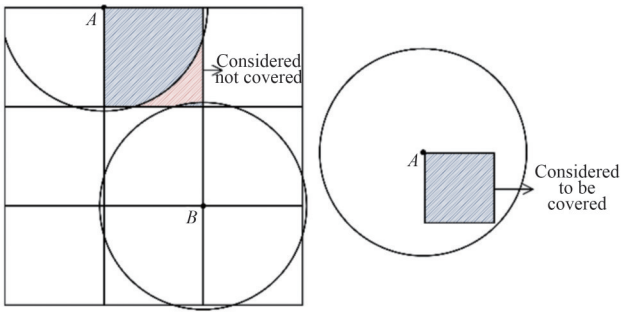


Figure 2 Coverage schematic

The mathematical expression is as follows:

$$f(x,y,z)=\begin{cases}1, & \text{if } \exists i\in \boldsymbol{X} \text{ such that } \forall v_j\in \boldsymbol{V}_{x,y,z},\ d(i,v_j)\leqslant r\\ 0, & \text{otherwise}\end{cases} \tag{12}$$

If the monitoring space is divided into $n_1\times n_2\times n_3$ cubes, then $f(x,y,z)$ indicates whether the cube at (x,y,z) is covered. $\boldsymbol{X}$ refers to the set of coordinates of all sensor nodes in the network, and $\boldsymbol{V}_{x,y,z}$ represents the set of all vertices of the cube at (x,y,z). A cube is considered covered only if it is completely protected by at least one node (Jin et al., 2019). Thus, the coverage rate r_{cov} can be calculated as follows:

$$r_{\text{cov}}=\frac{\sum_{x\in n_1,\,y\in n_2,\,z\in n_3} f(x,y,z)}{n_1\times n_2\times n_3} \tag{13}$$

Network resilience can be defined as the network's capability to resist damage to some extent. In sink-oriented network architectures, the topological implication of individual nodes exhibits substantial heterogeneity. Aiming to enhance network resilience, the traffic burden across nodes is implicitly equalized through structural homogenization, which involves balancing the importance of nodes within the network. This approach ensures that, even in the presence of random node expirations, the network can maintain excellent overall performance.

As mentioned in Section 2.1, BC can be used to describe the importance of nodes in networks. The standard deviation of BC can be minimized to balance the importance of nodes. The expression is presented as follows:

$$\text{BC}_{\text{std}}=\sqrt{\frac{\sum_{i=1}^{n}\left(\text{BC}_i-\overline{\text{BC}}\right)^2}{n-1}} \tag{14}$$

Based on the aforementioned, the fitness function can be expressed as shown below.

$$\text{fitness}=\alpha\cdot r_{\text{cov}}+(1-\alpha)\cdot \text{BC}_{\text{std}} \tag{15}$$

4 Numerical simulation

In this section, the effectiveness of the proposed DSR–VFPSO algorithm is verified via comparison with other existing algorithms, such as VFPSO, PSO, and random deployment. Liu et al. (2019) introduced the VFPSO algorithm, and its objective function is to maximize coverage. PSO refers to a simple PSO algorithm proposed by Ghosh et al. (2012), with a fitness function that also aims to maximize coverage. Aiming to further illustrate the advantages of the proposed hybrid algorithms, the results of a simple PSO algorithm, with coverage and BC as fitness functions, are also calculated. The random deployment algorithm randomly deploys nodes in the target area.

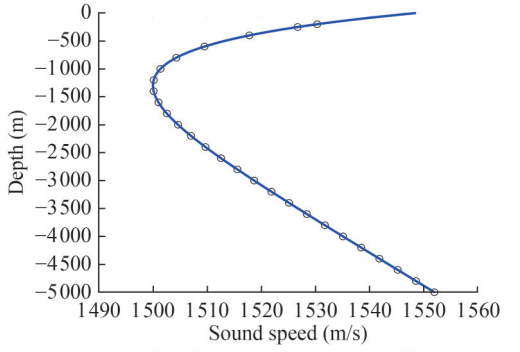
Aiming to evaluate resilience enhancement, node expirations due to adverse ocean environments are artificially simulated by randomly deleting nodes. Specifically, when a node fails, all links connected to the node also fail. This phenomenon can be summarized as the permanent independent random node failure model (Kong and Yeh, 2010). Permanent indicates that once the node fails, recovery is impossible (Huang et al., 2015). Random indicates that the probability and combination of node failures are both random. Independent indicates that the probability of node failure is independent and unaffected by other nodes.

4.1 Simulation setup

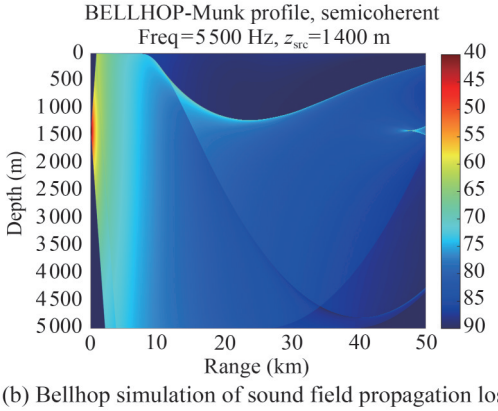
n nodes are deployed within an area of 5 km × 5 km × d km. The simulated sea area is the classic Munk deep-sea sound channel (Porter and Bucker, 1987), under which the sound speed profile and transmission loss diagram of the Bellhop-simulated sound field are shown in Figure 3.

The channel axis is located at a depth of 1 400 m; thus, d is set to 1400 m. The scenario involves optimizing the topology for cross-layer transmission among nodes in the shallow layers of the deep sea. The settings for the other parameters in this simulation are detailed in Table 1.

As discussed in Section 3.3, the experiment area must be divided into several mesh regions to calculate the coverage rate of the network. The parameter "Mesh size" in the table represents the size of each mesh body. As previously mentioned, this experiment simulates node expirations caused by the external conditions of the deep-sea environ-



(a) Munk-sound speed profile



(b) Bellhop simulation of sound field propagation loss

Figure 3 Bellhop sound channel simulation

Table 1 Simulation parameter setting

Parameters	Values
Sound source frequency (Hz)	5 500
Depth of deep-sea (m)	5 000
Seabed sound speed (m/s)	1 600
Seabed density (g/cm³)	1.8
Seabed attenuation coefficient (dB/λ)	0.8
Experimental area (x, y, z) (m)	(5 000, 5 000, 1 400)
Mesh size (x, y, z) (m)	(100, 100, 100)
Communication radius R_c (m)	1 500
Sensing radius R_s (m)	750
Weight of fitness function α	0.2
Individual learning factor c_1	0.45
Group learning factor c_2	0.45
Acceleration element c_3	0.45
MaxStep	1/2 R_s
Number of repeats	200

ment through the random deletion of nodes. Aiming to ensure the reliability of the results, the "random deletion" step is repeated multiple times, and the results are averaged to eliminate any bias. The "Number of repeats" in the last row of Table 1 indicates the number of repetitions for the "random deletion" step.

The simulation verification of the resilience of DSASN in this section is mainly divided into two parts: 1) Network invulnerability, which is assessed by comparing network coverage and connectivity before and after node failure, and 2) Energy consumption, which is measured by the number of rounds until the first node in the network fails.

Aiming to further improve the effectiveness of the DSR–VFPSO algorithm, the initial coverage of the network is also compared to ensure that its initial performance remains excellent while improving the resilience.

4.2 Network invulnerability

The application scenario in this paper focuses on topology optimization before actual deployment. Therefore, the connectivity and coverage rates of the network after partial node failure directly measure the invulnerability of the network to attacks. Maintaining high connectivity and coverage rates indicates that the network is highly fault-tolerant and exhibits good resilience.

The abnormal failure scenario of underwater network nodes in deep-sea environments is simulated via the random deletion of nodes in the network.

The number of nodes in the simulation is 20. Aiming to comprehensively assess algorithmic performance, comparative analyses between the proposed method and other algorithms, including VFPSO, simple PSO, PSO with proposed fitness function ("PSO with BC" in figures), genetic algorithm (GA) with proposed fitness function ("GA with BC" in figures), are conducted to effectively demonstrate thecompetitive advantages of DSR–VFPSO. The results are presented in Figures 4 and 5. The formulas for calculating the connectivity and coverage rates are shown in Eqs. (11) and (13), respectively.

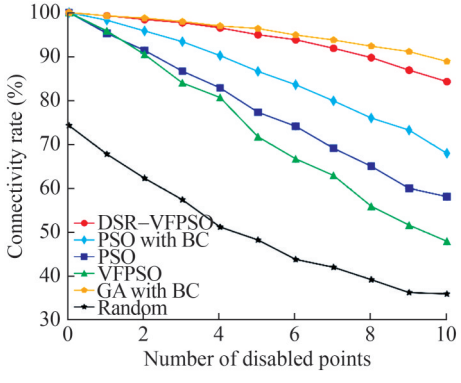


Figure 4 Connectivity change curve after node failure

Notably, at the beginning, except for the random deployment algorithm, the connectivity rate of other algorithms is 100%. When the number of failed nodes increases, the connectivity rate gradually decreases. The connectivity retention rate of the proposed algorithm is slightly lower than that of GA but higher than that of other algorithms.

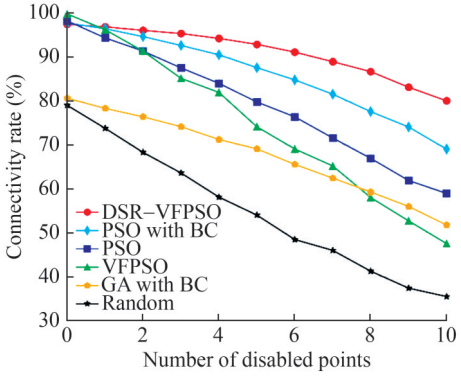


Figure 5 Coverage change curve after node failure

After node failure (taking 10 nodes as an example), the connectivity rate of the DSR–VFPSO algorithm is 16.34%, 26.20%, 36.35%, and 48.33% higher than that of PSO with BC, PSO, VFPSO, and random deployment, respectively, and 4.58% lower than GA with BC.

In terms of coverage, as the number of failed nodes increases, the coverage rate also gradually decreases. Although the initial coverage of the proposed DSR–VFPSO algorithm is slightly lower than that of the VFPSO and PSO algorithms, its coverage after node failure is higher than other algorithms. Take 10 nodes that fail as an example. After node failure, the coverage rates of DSR–VFPSO, PSO with BC, PSO, VFPSO, GA with BC, and random deployment are 17.43%, 28.75%, 39.32%, 52.33%, 28.89%, and 43.57% lower than their initial values, respectively.

These results are expected. The DSR–VFPSO algorithm, PSO with BC, and GA with BC consider BC (which is the index considered for enhancing resilience), while the remaining three overlook this parameter. Therefore, after random node expirations, the DSR–VFPSO demonstrates excellent connectivity and coverage preservation performance. By combining the advantages of VFA and PSO, the DSR–VFPSO outperforms the basic PSO with BC. In comparison to GA with BC, although it achieves higher connectivity preservation after node failures, DSR–VFPSO has superior initial coverage and coverage retention rates. Figure 6 shows one of the topological solutions generated by each algorithm. Noatbly, GA maintains high connectivity due to its relatively compact node deployment, which leads to a lower area coverage. A possible explanation is that GA may get trapped in local optima, thereby failing to achieve the optimal spatial distribution of nodes.

Based on the preceding analysis, the DSR–VFPSO algorithm exhibits superior survivability compared to the benchmark algorithms.

4.3 Energy consumption

The energy consumption during data transmission and retrieval is calculated based on the energy consumption model described in Section 2.3. When a node is heavily loaded, its energy tends to deplete quickly. In DSASNs with sink nodes, the failure of a heavily loaded node often makes it challenging for the network to complete its tasks effectively. Therefore, in this paper, network lifetime is the number of cycles at which the first node dies due to energy exhaustion (Dong et al., 2020). After partial node

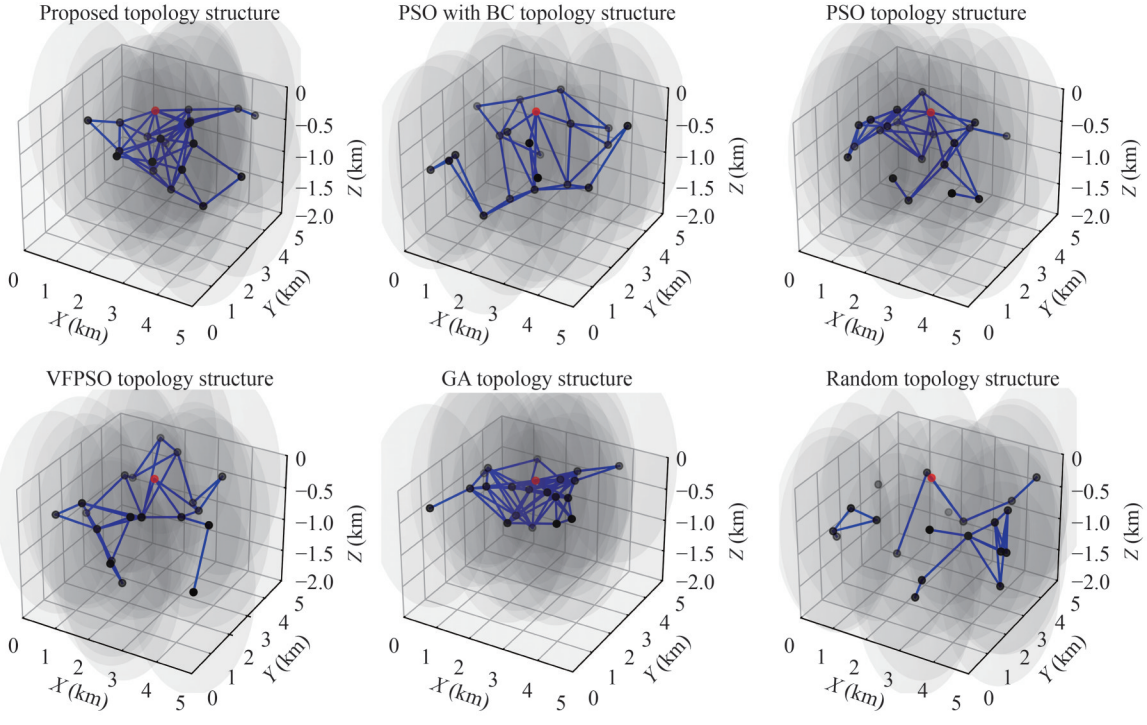


Figure 6 Topology structure of each algorithm

failure, a longer time that the first node continues to function indicates that the network has good energy efficiency and energy management capabilities, thereby indicating strong resilience.

In this part of the simulation, the routing protocol used is the minimum hop routing protocol. A path is randomly selected in the presence of multiple paths with the same hops.

The network energy consumption under different algorithms is compared by setting various loads. The network load is represented by setting the probability and using the Poisson distribution to generate tasks. The following expression simulates the number of tasks that occur per second in 100 s.

$$a_i \sim \text{Poisson}(\text{task_load}),\ i = 1, 2, 3, \cdots, 100 \qquad (16)$$

where a_i is a random variable of the Poisson distribution, representing the number of tasks that occur in a given second, and task_load is the average number of packets per second. According to Eq. (16), random numbers are generated based on a given task_load probability to simulate the network load. Only a_i values greater than 0 are considered, representing the number of active tasks in the network under the load of task_load. These tasks are then randomly assigned to nodes in the network to simulate task allocation. Based on this setup, the simulation calculates the corresponding energy consumption.

The energy consumption results for the DSR–VFPSO, PSO with BC, PSO, VFPSO, and GA with BC algorithms are shown in Figure 7. The random deployment algorithm is excluded from the comparison because it cannot ensure full network connectivity.

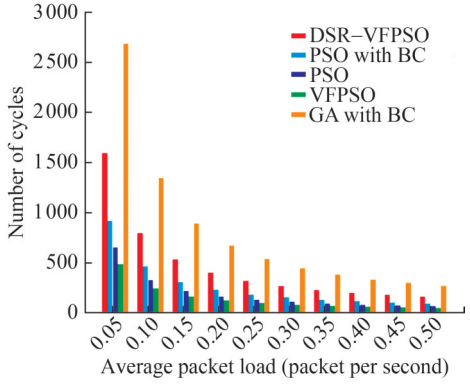


Figure 7 Energy consumption comparison

Notably, the network lifetime decreases as the load increases. Among the compared algorithms, the GA achieves an extended network lifetime due to its compact deployment, which facilitates multiple routing paths. However, excluding GA, DSR–VFPSO outperforms the other three algorithms in terms of operational lifetime. When the load is 0.05, the lifetime of DSR–VFPSO is nearly twice that of VFPSO and PSO, and approximately 1.5 times longer than PSO with BC. These results highlight the strong performance of the DSR–VFPSO algorithm.

Additionally, to account for variations in network scale, a comparative analysis of energy consumption across different network sizes (node counts) is conducted, all with an average packet load of 0.25. As illustrated in Figure 8, the results are consistent with the performance trends observed in the 20-node scenario.

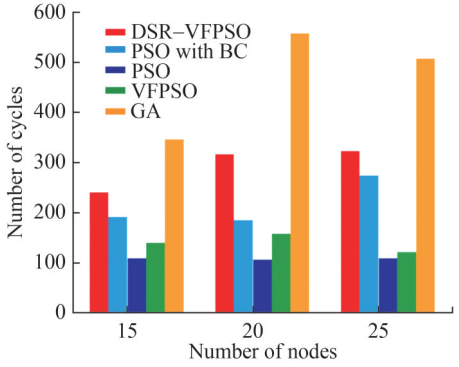


Figure 8 Energy consumption comparison across different network sizes

4.4 Initial coverage

Comparative results from Sections 4.2 and 4.3 reveal that the resilience of DSR–VFPSO notably surpasses that of the other algorithms. This section further evaluates the performance of the DSR–VFPSO algorithm by comparing initial coverage against the number of deployed nodes.

The formula for calculating coverage rate is given in Eq. (13). Herein, the proposed DSR–VFPSO algorithm is compared with PSO with BC, PSO, VFPSO, and GA with BC. Experiments are conducted within the same area, using identical iteration counts while varying the number of deployed nodes. The coverage comparison results are shown in Figure 9.

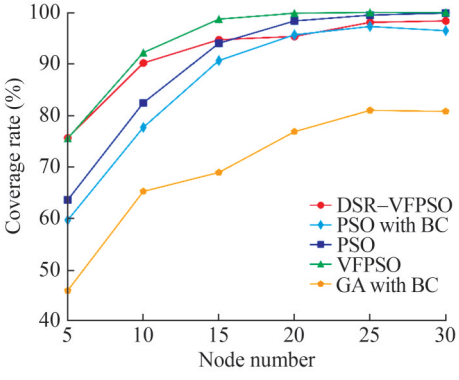


Figure 9 Coverage comparison result figure

Notably, as the number of nodes increases, the coverage rate of the experimental area constantly improves. When

the node count is low, the algorithm incorporating VFA achieves a higher coverage rate compared to the PSO algorithm alone. As the number of nodes increases, all algorithms except GA with BC reach final coverage rates above 95%. Among all the compared algorithms, VFPSO demonstrates excellent performance in maximizing coverage. The coverage results for DSR–VFPSO and PSO with BC are slightly lower than those of VFPSO and PSO, possible due to their multi-objective optimization approach. However, DSR–VFPSO outperforms PSO with BC, further highlighting the advantages of the hybrid DSR–VFPSO algorithm.

5 Conclusions

In this paper, the issues of sensor node energy limitations, unstable connectivity quality, and abnormal node failures in DSASN are addressed by proposing a three-dimensional hybrid topology optimization algorithm, DSR–VFPSO, which integrates VFA and PSO to improve the resilience of DSASNs. Unlike similar studies on shallow water acoustic networks, the proposed algorithm considers the influence of deep-sea sound shadow zones in cross-layer transmission and combines VFA and PSO to find the optimal topology that maximizes network coverage and resilience while ensuring full connectivity of the DSASN with the sink node. Numerical simulation results, obtained by artificially imposing random node expirations on a simulated deep-sea network to mimic the impact of adverse marine environments, show that the proposed DSR–VFPSO algorithm achieves better invulnerability and longer lifetime than other comparison algorithms while maintaining a high coverage rate. Future work will focus on developing dynamic topology reconfiguration mechanisms with embedded real-time responsiveness, coupled with AI-based predictive failure models, thereby allowing data-informed topology adjustments in mission-critical marine environments.

Competing interests Feng Tong is an editorial board member for the Journal of Marine Science and Application and was not involved in the editorial review, or the decision to publish this article. All authors declare that there are no other competing interests.

References

Akyildiz IF, Pompili D, Melodia T (2005) Underwater acoustic sensor networks: research challenges. Ad Hoc Networks 3: 257-279. https://doi.org/10.1016/j.adhoc.2005.01.004

Annapurna R, Sudhir AC (2023) Multi-population firefly algorithm based node deployment in underwater wireless sensor networks. Wireless Personal Communications 130(1): 635-649. https://doi.org/10.1007/s11277-023-10303-9

Awan KM, Shah PA, Iqbal K, Gillani SA, Ahmad W, Nam Y (2019) Underwater wireless sensor networks: a review of recent issues and challenges. Wirel. Commun. Mob. Comput. 6470359: 1-20. https://doi.org/10.1155/2019/6470359

Chi Y, Lin C, Tian Y, Wang L (2023) Flexible topological control for underwater optical wireless sensor networks. IEEE 43rd International Conference on Distributed Computing Systems (ICDCS), Hong Kong, China, 429-439. https://doi.org/10.1109/icdcs57875.2023.00061

Dong M, Li H, Li C, Hu Y, Huang H (2023) Energy-efficient sensor deployment strategy for optimal coverage of underwater events inspired by Krill Herd. IEEE Transactions on Industrial Informatics 20(3): 3900-3912. https://doi.org/10.1109/TII.2023.3316212

Dong M, Li H, Li Y, Deng Y, Yin R (2020) Fault-tolerant topology with lifetime optimization for underwater wireless sensor networks. Sādhanā 45: 1-8. https://doi.org/10.1007/s12046-020-01406-1

Dong M, Li H, Yin R, Qin Y, Hu Y (2022) Energy-saving and fault-tolerant topology for underwater acoustic sensor networks. OCEANS, Virginia, USA, 1-5. https://doi.org/10.1109/oceans47191.2022.9977158

Freeman LC (1977) A set of measures of centrality based on betweenness. Sociometry 40(1): 35-41. https://doi.org/10.2307/3033543

Ghosh S, Das S, Kundu D, Suresh K, Abraham A (2012) Inter-particle communication and search-dynamics of best particle swarm optimizers: An analysis. Inf. Sci. 182: 156-168. https://doi.org/10.1016/j.ins.2010.10.015

Hong Z, Pan X, Chen P, Su X, Wang N, Lu W (2018) A topology control with energy balance in underwater wireless sensor networks for IoT-based application. Sensors 18(7): 2306. https://doi.org/10.3390/s18072306

Hu Y, Sun YJ, Chen LQ (2022) The VF-PSO optimization algorithm for coverage and deployment of underwater wireless sensor network. Indian Journal of Geo-Marine Sciences 51(3): 219-228. https://doi.org/10.56042/ijms.v51i03.33392

Huang Y, Martínez J, Sendra J, López-Santidrián L (2015) Resilient wireless sensor networks using topology control: a review. Sensors (Basel, Switzerland) 15: 24735-24770. https://doi.org/10.3390/s151024735

Jin H, Liu B, Chen W, Ling J (2019) Research on the nodes deployment scheme for sensor coverage in underwater wireless networks based on genetic algorithm. Chinese Journal of Sensors and Actuators 32(7): 1083-1087. (in Chinese). https://doi.org/10.3969/j.issn. 1004-1699.2019.07.021

Kong Z, Yeh M (2010) Resilience to degree-dependent and cascading node failures in random geometric networks. IEEE Transactions on Information Theory 56(11): 5533-5546. https://doi.org/10.1109/TIT.2010.2068910

Kumar Gola K, Chaurasia N, Gupta B, Singh Niranjan D (2021) Sea lion optimization algorithm based node deployment strategy in underwater acoustic sensor network. International Journal of Communication Systems 34(5): e4723. https://doi.org/10.1002/dac.4723

Li D, Wang W, Li Y, Li S, Yu X (2024) Cluster restricted despreading method of long-range pilot-free orthogonal multicarrier spread spectrum communication in deep sea. ACTA ACUSTICA (4): 753-763. (in Chinese). https://doi.org/10.12395/0371-0025.2024091

Liu C, Zhao Z, Qu W, Qiu T, Sangaiah AK (2019) A distributed node deployment algorithm for underwater wireless sensor networks based on virtual forces. J. Syst. Archit. 97: 9-19. https://doi.org/10.1016/j.sysarc.2019.01.010

Porter MB, Bucker HP (1987) Gaussian beam tracing for computing ocean acoustic fields. The Journal of the Acoustical Society of

America 82(4): 1349-1359. https://doi.org/10.1121/1.395269

Preisig J (2007) Acoustic propagation considerations for underwater acoustic communications network development. ACM Sigmobile Mobile Computing & Communications Review 11(4): 2-10. https://doi.org/10.1145/1347364.1347370

Sandeep DN, Kumar V (2017) Review on clustering, coverage and connectivity in underwater wireless sensor networks: A communication techniques perspective. IEEE Access 5: 11176-99. https://doi.org/10.1109/ACCESS.2017.2713640

Sterbenz JP, Hutchison D, Çetinkaya EK, Jabbar A, Rohrer JP, Schöller M, Smith P (2014) Redundancy, diversity, and connectivity to achieve multilevel network resilience, survivability, and disruption tolerance invited paper. Telecommunication Systems 56: 17-31. https://doi.org/10.1007/s11235-013-9816-9

Sun Y, Hu Y, Chen L, Liu H, Chen J, Lv B (2020) The coverage optimization method for underwater sensor network based on VF-PSO algorithm. Chinese Control and Decision Conference (CCDC), Hefei, China, 2008-2013. https://doi.org/10.1109/CCDC49329.2020.9164708

Vihman L, Kruusmaa M, Raik J (2021) Systematic review of fault tolerant techniques in underwater sensor networks. Sensors 21(9): 3264. https://doi.org/10.3390/s21093264

Wang X, Wang S, Bi D (2007) Virtual force-directed particle swarm optimization for dynamic deployment in wireless sensor networks. Advanced Intelligent Computing Theories and Applications. With Aspects of Theoretical and Methodological Issues: Third International Conference on Intelligent Computing, ICIC, Qingdao, China, 292-303. https://doi.org/10.1007/978-3-540-74171-8_29

Xu C, Song S, Liu J, Xu Y, Che S, Lin B, Xu G (2023) An efficient deployment scheme with network performance modeling for underwater wireless sensor networks. IEEE Internet of Things Journal 11(5): 8345-8359. https://doi.org/10.1109/JIOT.2023.3318222

Yan L, He Y, Huangfu Z (2021) An uneven node self-deployment optimization algorithm for maximized coverage and energy balance in underwater wireless sensor networks. Sensors 21(4): 1368. https://doi.org/10.3390/s21041368

Yuan Y, Shen X, Sun L, He K, Wang H (2024) Modeling cascading failures and invulnerability analysis of underwater acoustic sensor networks based on complex network. IEEE Sensors Journal 24: 6942-6952. https://doi.org/10.1109/JSEN.2024.3350356

Zhao Y, Tong F, Ma B, Zhou Y, Yang X (2024) Multipath-cluster-wise joint equalization method for long-range deep-sea single-element underwater acoustic communication. ACTA ACUSTICA (4): 764-773. (in Chinese). https://doi.org/10.12395/0371-0025.2024038